Emulation of *n*-photon Jaynes-Cummings and anti-Jaynes-Cummings models via parametric modulation of a cyclic qutrit

A. V. Dodonov,[1,*] A. Napoli,[2,3] and B. Militello[2,3]

[1]*Institute of Physics and International Centre for Condensed Matter Physics, University of Brasilia, 70910-900 Brasilia, Federal District, Brazil*

[2]*Dipartimento di Fisica e Chimica-Emilio Segrè, Università degli Studi di Palermo, Via Archirafi 36, I-90123 Palermo, Italy*

[3]*INFN Sezione di Catania, Via Santa Sofia 64, I-95123 Catania, Italy*

We study a circuit QED setup involving a single cavity mode and a cyclic qutrit whose parameters are time modulated externally. It is shown that in the dispersive regime this system behaves as a versatile platform to implement effective *n*-photon Jaynes-Cummings (JC) and anti-Jaynes-Cummings (AJC) models by suitably setting the modulation frequency. The atomic levels and the cavity Fock states involved in the effective Hamiltonians can be controlled through adjustment of the system parameters, and different JC and AJC interactions can be implemented simultaneously using multitone modulations. Moreover, one can implement some models that go beyond simple JC and AJC-like interaction, such as multiphoton coupling between certain entangled states. We estimate analytically the associated transition rates and study numerically the dynamics in the presence of Markovian dissipation, demonstrating that lower-order effective Hamiltonians can be implemented with current technology.

I. INTRODUCTION

The Jaynes-Cummings (JC) Hamiltonian [1] is probably the most famous and fundamental model in the context of radiation-matter interaction. It involves a cavity mode (or a generic quantum harmonic oscillator) coupled to a two-level atom (or a generic two-state system). Such a model describes coherent transitions between the two systems, where every upward (downward) atomic transition is accompanied by the loss (acquisition) of a photon. The complementary model describing simultaneous upward atomic transitions and photon acquisition is known as the anti-Jaynes-Cummings (AJC) Hamiltonian. Both models descend from the quantum Rabi model (QRM) [2] under suitable hypotheses concerning the characteristic frequencies of the two subsystems, the strength of their coupling, and external drivings, which allow for the rotating-wave approximation (RWA). Beyond this limit, the QRM is difficult to solve and the diagonalization of the corresponding Hamiltonian has been an open problem for decades. Only in the last few years some papers appeared where analytic resolutions of the QRM were proposed [2–4].

The importance of the QRM and its approximated versions goes beyond the physical context of cavity quantum electrodynamics (QED). Indeed, JC and AJC models are widely used in the effective description of trapped ions [5], while QRM spontaneously emerges in the circuit QED context [6–10], where it can be implemented also in the ultrastrong regime [11–14] (which implies the impossibility to reduce the original model to the JC model or the AJC model). Depending on the coupling strengths and the resonances involving the

two subsystems, multiphoton JC, AJC, and Rabi models can be implemented [15]. The nonlinear generalizations of the QRM, in particular the two-photon QRM, have very recently attracted attention also in view of its potential application to platforms exploited for quantum technologies [16–19].

Interesting applications of the QRM are obtained when the relevant Hamiltonian becomes time dependent. Generally speaking, though time-dependent Hamiltonians are difficult to solve analytically unless specific conditions are satisfied [20–23], several classes of time-dependent Hamiltonians that are approximately solvable can be identified, such as those related to phenomena ranging from Landau-Zener processes [24–32] to STIRAP manipulation [33–39] to periodically driven systems [40–42].

Specific to the Rabi model, when some parameters turn out to be time dependent, a significant amount of photons can be produced from vacuum (and other initial states) in the so-called dynamical Casimir effect (DCE) [32,43–45], when the photons are generated in pairs while the atomic populations remain nearly unaffected. Conversely, photons can be coherently annihilated from certain initial states due to resonant external modulations. The term antidynamical Casimir effect (ADCE) was originally coined to describe such annihilation of three photons in the dispersive regime of QRM [45–47], which resembles formally the three-photon JC model with a Kerr nonlinearity. Moreover, it was recently shown that the rate of ADCE can be substantially increased by employing qutrits [48], while a cyclic qutrit allows for realization of novel effects, such as one- and three-photon DCEs [49]. So here we investigate whether a cyclic qutrit could be used to implement multiphoton JC and AJC effective interactions by suitably modulating the energy levels. It is found that this task is indeed feasible, and in addition our scheme permits

*adodonov@fis.unb.br

the implementation of combined models (superpositions of JC and AJC interaction terms) and other multiphoton transitions between entangled atom-cavity states. This fact effectively implies the possibility of manipulating the degree of entanglement of the system and, in particular, generating entangled states. To better bring to light this possibility, we analyze the time behavior of the logarithmic negativity [50], which is an evolution of the standard negativity [51,52].

The paper is organized as follows. In Sec. II we introduce the physical system, consisting of a cyclic qutrit coupled to a single cavity mode and show that in the dispersive regime it can be used as a versatile platform to emulate multiphoton JC and AJC interactions between any pair of atomic levels. In Sec. III numerical results are reported, attesting that under resonant modulation of atomic levels the exact system dynamics is essentially equivalent to the effective description in terms of multiphoton JC and AJC models. We also estimate the effects of dephasing and relaxation using a phenomenological master equation, analyzing which transitions are less susceptible to dissipation. In Sec. IV we consider the regime of parameters for which the system bare eigenstates consist of entangled qutrit-cavity states. It is shown that in this "hybrid" regime the four-photon JC transitions become substantially faster (hence more robust against quantum noise) and novel three-photon transitions can occur between the entangled atom-field states. Finally, Sec. V contains our main conclusions.

II. PHYSICAL SYSTEM

We consider a single cavity mode of constant frequency ω that interacts with a qutrit in the cyclic configuration [10,53–56], so that all the atomic transitions are allowed via one-photon transitions. The Hamiltonian reads

$$
\hat{H}/\hbar = \omega\hat{n} + \sum_{k=1}^{2} E_k(t)\hat{\sigma}_{k,k}
$$
$$
+ \sum_{k=0}^{1}\sum_{l>k}^{2} g_{k,l}(\hat{a} + \hat{a}^\dagger)(\hat{\sigma}_{l,k} + \hat{\sigma}_{k,l}). \quad (1)
$$

Here $\hat{a}$ ($\hat{a}^\dagger$) is the cavity annihilation (creation) operator and $\hat{n} = \hat{a}^\dagger\hat{a}$ is the photon number operator. The atomic levels are $E_0 \equiv 0$, E_1, and E_2, the corresponding states are denoted as $|\mathbf{k}\rangle$, and we define $\hat{\sigma}_{k,j} \equiv |\mathbf{k}\rangle\langle\mathbf{j}|$. The constant parameters $g_{k,l}$ denote the coupling strengths between the atomic states $|\mathbf{k}\rangle$ and $|\mathbf{l}\rangle$ mediated by the cavity field. To emphasize the role of the counter-rotating terms (CRT) we rewrite (for $l > k$)

$$
g_{k,l}(\hat{a} + \hat{a}^\dagger)(\hat{\sigma}_{l,k} + \hat{\sigma}_{k,l}) \rightarrow g_{k,l}(\hat{a}\hat{\sigma}_{l,k} + c_{k,l}\hat{a}\hat{\sigma}_{k,l} + \text{H.c.}),
$$

where $c_{k,l} = 1$ when the corresponding CRT is taken into account and is zero otherwise (in our numeric examples we consider $c_{k,l} = 1 \,\forall\, k, l$). Moreover, to shorten the final expressions we define $g_1 \equiv g_{0,1}$, $g_2 \equiv g_{1,2}$, and $g_3 = g_{0,2}$, and similarly for c_1, c_2, and c_3.

Utilizing the tunability of Josephson artificial atoms [57–63], we assume that the atomic energy levels can be modulated externally via multitone driving as

$$
E_k(t) \equiv E_k^{(0)} + \varepsilon_k f_k, \quad f_k = \sum_j w_k^{(j)}\sin\left(\eta^{(j)}t + \phi_k^{(j)}\right),
$$

where $\varepsilon_k \ll E_k^{(0)}$ is the modulation depth and $\hbar E_k^{(0)}$ is the bare energy value ($k = 1$ or 2). The sum runs over all the input frequencies $\eta^{(j)}$, and $w_k^{(j)}$ ($\phi_k^{(j)}$) is the associated weight (phase) [64].

We expand the wave function as

$$
|\psi(t)\rangle = \sum_{n}^{\infty} e^{-it\lambda_n} b_n(t)\mathcal{F}_n(t)|\varphi_n\rangle,
$$

$$
\mathcal{F}_n(t) = \exp\left\{\sum_{k=1}^{2}\sum_j \frac{i\varepsilon_k w_k^{(j)}}{\eta^{(j)}}\langle\varphi_n|\hat{\sigma}_{k,k}|\varphi_n\rangle\right.
$$

$$
\left.\times\left[\cos\left(\eta^{(j)}t + \phi_k^{(j)}\right) - \cos\left(\phi_k^{(j)}\right)\right]\right\}. \quad (2)
$$

Here λ_n are the eigenfrequencies of the bare Hamiltonian $\hat{H}_0 \equiv \hat{H}[\varepsilon_1 = \varepsilon_2 = 0]$ (n increasing with energy) and $|\varphi_n\rangle$ are the corresponding eigenstates (dressed states). $b_n(t)$ denotes the slowly varying probability amplitude of the state $|\varphi_n\rangle$ and $\mathcal{F}_n(t) \approx 1$ is a rapidly oscillating function.

After substituting Eq. (2) into the Schrödinger equation, assuming that $\varepsilon_k w_k^{(j)}\langle\varphi_m|\hat{\sigma}_{k,k}|\varphi_n\rangle \ll \eta^{(j)}$ and that $|\eta^{(j)} \pm \eta^{(r)}| \neq |\lambda_n - \lambda_m|$ for all possible values of k, r, j, n, and m, to the first order in ε_1 and ε_2 we obtain the coupled differential equations

$$
\dot{b}_m = \sum_j\sum_{n<m} \Theta_{n;m}^{(j)*}\exp[it(|\lambda_n - \lambda_m| - \eta^{(j)})]b_n
$$

$$
- \sum_j\sum_{n>m} \Theta_{m;n}^{(j)}\exp[-it(|\lambda_n - \lambda_m| - \eta^{(j)})]b_n, \quad (3)
$$

where to the lowest order

$$
\Theta_{m;n}^{(j)} = \sum_{k=1}^{2} \frac{\varepsilon_k^{(j)}}{2}\langle\varphi_m|\hat{\sigma}_{k,k}|\varphi_n\rangle, \quad \varepsilon_k^{(j)} \equiv \varepsilon_k w_k^{(j)}\exp\left(i\phi_k^{(j)}\right).
$$

We see that for the modulation frequency $\eta^{(\text{res})} = |\lambda_n - \lambda_m|$ the dressed states $|\varphi_n\rangle$ and $|\varphi_m\rangle$ become resonantly coupled with the ideal transition rate $|\Theta_{m;n}^{(\text{res})}|$. Indeed, assuming that all other transitions are strongly off-resonant, we obtain $|\dot{b}_m| = |\Theta_{m;n}^{(\text{res})}b_n|$ and a similar expression for $|\dot{b}_n|$. However, some undesirable nonresonant transitions (for which $|\lambda_k - \lambda_l - \eta^{(\text{res})}| \lesssim |\Theta_{k;l}^{(\text{res})}|$) still take place, decreasing the effective (average) value of b_n on the right-hand side, thereby lowering the actual transition rate between the dressed states $|\varphi_n\rangle$ and $|\varphi_m\rangle$. Therefore, when the analytic description is oversimplified by restricting the dynamics to the truncated subspace $\{|\varphi_n\rangle, |\varphi_m\rangle\}$, $|\Theta_{m;n}^{(j)}|$ provides only the order of magnitude for the corresponding transition rate. Nonetheless, it is crucial to have closed analytic expressions for $|\Theta_{m;n}^{(j)}|$ to understand how it scales with the detunings and coupling strengths.

First we consider the dispersive regime, so that the atomic populations remain nearly constant in the absence of external modulation. We require $\omega \gg |\Delta_1|, |\Delta_2|, |\Delta_3| \gg \sqrt{n_{\max}}\max(g_k)$, where $n_{\max}$ is the maximum number of the system excitations and the bare detunings are defined as

$$
\Delta_1 \equiv \omega - E_1^{(0)}, \quad \Delta_2 \equiv \omega - \left(E_2^{(0)} - E_1^{(0)}\right), \quad \Delta_3 \equiv \Delta_1 + \Delta_2.
$$

In this regime the dressed states read $|\beta_{k,n}\rangle = \mathcal{N}_{k,n}[|\mathbf{k}, n\rangle + \sum_{l=1}^{\infty}|\mathbf{k}, n\rangle_{(l)}]$, where $|n\rangle$ is the cavity Fock state and $|\mathbf{k}, n\rangle_{(l)}$ denotes the lth order correction obtained

from the perturbation theory ($\mathcal{N}_{k,n}$ is the normalization constant). To the lowest order the corresponding eigenfrequencies are

$$\lambda_{0,k} \approx \omega k + \frac{g_1^2 k}{\Delta_1} - \frac{c_1 g_1^2 (k+1)}{2\omega - \Delta_1} - \frac{g_3^2 k}{\omega - \Delta_3}$$
$$- \frac{c_3 g_3^2 (k+1)}{3\omega - \Delta_3} + \frac{k g_1^2}{\Delta_1^2}\left(\frac{g_2^2(k-1)}{\Delta_3} - \frac{g_1^2 k}{\Delta_1}\right), \quad (4)$$

$$\lambda_{1,k} \approx \omega(k+1) - \Delta_1 - \frac{g_1^2(k+1)}{\Delta_1} + \frac{c_1 g_1^2 k}{2\omega - \Delta_1}$$
$$+ \frac{g_2^2 k}{\Delta_2} - \frac{c_2 g_2^2(k+1)}{2\omega - \Delta_2}$$
$$+ \left(\frac{g_1^2(k+1)}{\Delta_1^2} + \frac{g_2^2 k}{\Delta_2^2}\right)\left(\frac{g_1^2(k+1)}{\Delta_1} - \frac{g_2^2 k}{\Delta_2}\right), \quad (5)$$

$$\lambda_{2,k} \approx \omega(k+2) - \Delta_3 - \frac{g_2^2(k+1)}{\Delta_2} + \frac{c_2 g_2^2 k}{2\omega - \Delta_2}$$
$$+ \frac{g_3^2(k+1)}{\omega - \Delta_3} + \frac{c_3 g_3^2 k}{3\omega - \Delta_3}$$
$$- \frac{g_2^2(k+1)}{\Delta_2^2}\left(\frac{g_1^2(k+2)}{\Delta_3} - \frac{g_2^2(k+1)}{\Delta_2}\right). \quad (6)$$

The first-order corrections to the eigenstates read

$$|\mathbf{0},k\rangle_{(1)} = \frac{g_1\sqrt{k}}{\Delta_1}|\mathbf{1},k-1\rangle - \frac{c_1 g_1\sqrt{k+1}}{2\omega - \Delta_1}|\mathbf{1},k+1\rangle$$
$$- \frac{c_3 g_3\sqrt{k+1}}{3\omega - \Delta_3}|\mathbf{2},k+1\rangle - \frac{g_3\sqrt{k}}{\omega - \Delta_3}|\mathbf{2},k-1\rangle, \quad (7)$$

$$|\mathbf{1},k\rangle_{(1)} = \frac{c_1 g_1\sqrt{k}}{2\omega - \Delta_1}|\mathbf{0},k-1\rangle - \frac{g_1\sqrt{k+1}}{\Delta_1}|\mathbf{0},k+1\rangle$$
$$- \frac{c_2 g_2\sqrt{k+1}}{2\omega - \Delta_2}|\mathbf{2},k+1\rangle + \frac{g_2\sqrt{k}}{\Delta_2}|\mathbf{2},k-1\rangle, \quad (8)$$

$$|\mathbf{2},k\rangle_{(1)} = \frac{c_3 g_3\sqrt{k}}{3\omega - \Delta_3}|\mathbf{0},k-1\rangle + \frac{g_3\sqrt{k+1}}{\omega - \Delta_3}|\mathbf{0},k+1\rangle$$
$$- \frac{g_2\sqrt{k+1}}{\Delta_2}|\mathbf{1},k+1\rangle + \frac{c_2 g_2\sqrt{k}}{2\omega - \Delta_2}|\mathbf{1},k-1\rangle,$$

and the complete expressions for the fourth-order shifts and $|\mathbf{k},n\rangle_{(2)}$ are summarized in Appendix A.

Equation (3) shows that after neglecting rapidly oscillating terms, the dispersive cyclic qutrit can serve as a versatile platform to emulate k-photon JC and AJC Hamiltonians between the atomic states $\{|\mathbf{l}\rangle, |\mathbf{j}\rangle\}$:

$$\hat{H}_{JC}^{(k)}(l,j) \equiv i\mathcal{J}_{l,j}^{(k)*}\hat{a}^{\dagger k}\hat{\sigma}_{l,j} + \text{H.c.} \quad (9)$$

$$\hat{H}_{AJC}^{(k)}(l,j) \equiv i\mathcal{A}_{l,j}^{(k)}\hat{a}^k\hat{\sigma}_{l,j} + \text{H.c.}, \quad (10)$$

where $j > l$ and $\mathcal{A}_{l,j}^{(k)}$ and $\mathcal{J}_{l,j}^{(k)}$ are the effective coupling strengths. These Hamiltonians hold approximately in the truncated subspace $\{|\mathbf{j},n\rangle, |\mathbf{l},n\pm k\rangle\}$, where n can be either a fixed integer or belong to a small domain ($n_1 \leqslant n \leqslant n_2$) depending on the parameters of the system [i.e., depending on which

arguments of the exponentials in Eq. (3) are nearly zero for a given modulation frequency $\eta^{(\text{res})}$]. To the lowest order one obtains the following:

(i) one-photon models:

$$\mathcal{J}_{0,1}^{(1)} \approx \varepsilon_1^{(r)}\frac{g_1}{2\Delta_1}, \quad \mathcal{A}_{0,1}^{(1)} \approx \varepsilon_1^{(r)}\frac{c_1 g_1}{2(2\omega - \Delta_1)},$$

$$\mathcal{J}_{1,2}^{(1)} \approx \left(\varepsilon_2^{(r)} - \varepsilon_1^{(r)}\right)\frac{g_2}{2\Delta_2}, \quad \mathcal{A}_{1,2}^{(1)} \approx \left(\varepsilon_2^{(r)} - \varepsilon_1^{(r)}\right)\frac{c_2 g_2}{2(2\omega - \Delta_2)},$$

$$\mathcal{J}_{0,2}^{(1)} \approx -\varepsilon_2^{(r)}\frac{g_3}{2(\omega - \Delta_3)}, \quad \mathcal{A}_{0,2}^{(1)} \approx \varepsilon_2^{(r)}\frac{c_3 g_3}{2(3\omega - \Delta_3)},$$

(ii) two-photon models:

$$\mathcal{J}_{0,1}^{(2)} \approx \left(\frac{\varepsilon_2^{(r)}}{2\omega - \Delta_2} - \frac{\varepsilon_1^{(r)}}{\omega + \Delta_1}\right)\frac{c_2 g_2 g_3}{2(\omega - \Delta_3)},$$

$$\mathcal{A}_{0,1}^{(2)} \approx \frac{c_3 g_2 g_3}{2(3\omega - \Delta_3)}\left(\frac{\varepsilon_2^{(r)}}{\Delta_2} - \frac{\varepsilon_1^{(r)}}{3\omega - \Delta_1}\right),$$

$$\mathcal{J}_{1,2}^{(2)} \approx \left(\frac{\varepsilon_2^{(r)}}{2\omega - \Delta_1} - \frac{\varepsilon_1^{(r)}}{\omega - \Delta_3}\right)\frac{c_1 g_1 g_3}{2(\omega + \Delta_2)},$$

$$\mathcal{A}_{1,2}^{(2)} \approx -\frac{c_3 g_1 g_3}{2(3\omega - \Delta_2)}\left(\frac{\varepsilon_1^{(r)}}{3\omega - \Delta_3} + \frac{\varepsilon_2^{(r)}}{\Delta_1}\right),$$

$$\mathcal{J}_{0,2}^{(2)} \approx \left(\frac{\varepsilon_2^{(r)}}{\Delta_3} - \frac{\varepsilon_1^{(r)}}{\Delta_2}\right)\frac{g_1 g_2}{2\Delta_1},$$

$$\mathcal{A}_{0,2}^{(2)} \approx \frac{c_1 c_2 g_1 g_2}{2(2\omega - \Delta_1)}\left(\frac{\varepsilon_1^{(r)}}{2\omega - \Delta_2} - \frac{\varepsilon_2^{(r)}}{4\omega - \Delta_3}\right). \quad (11)$$

Similarly one can obtain the coefficients $\mathcal{J}_{l,j}^{(k)}$ and $\mathcal{A}_{l,j}^{(k)}$ for three- and four-photon models, whose approximate expressions are summarized in Appendix B. Although these expressions provide only the upper bounds for the effective coupling strengths, they are crucial to identify the most advantageous regimes of parameters (e.g., when g_i/Δ_j appears instead of g_i/ω). It is worth noticing that one can also implement transitions $|\mathbf{l},n\rangle \leftrightarrow |\mathbf{j},n\rangle$ which do not alter the photon number. Introducing the effective Hamiltonian $\hat{H}_q^{(0)}(l,j > l) \equiv i\mathcal{S}_{l,j}(\hat{n})\hat{\sigma}_{l,j} + \text{H.c.}$, to the lowest order we find

$$\mathcal{S}_{0,1}(\hat{n}) \approx \frac{g_2 g_3}{2}\left[-\frac{\varepsilon_1^{(r)}}{\omega - \Delta_1}\left(\frac{\hat{n}}{\omega - \Delta_3} + \frac{c_2 c_3(\hat{n}+1)}{3\omega - \Delta_3}\right)\right.$$
$$\left. + \varepsilon_2^{(r)}\left(\frac{\hat{n}}{\Delta_2(\omega - \Delta_3)} - \frac{c_2 c_3(\hat{n}+1)}{(3\omega - \Delta_3)(2\omega - \Delta_2)}\right)\right],$$

$$\mathcal{S}_{1,2}(\hat{n}) \approx \frac{g_1 g_3}{2(\omega - \Delta_2)}\left[-\varepsilon_1^{(r)}\left(\frac{c_1 c_3 \hat{n}}{3\omega - \Delta_3} + \frac{\hat{n}+1}{\omega - \Delta_3}\right)\right.$$
$$\left. + \varepsilon_2^{(r)}\left(\frac{c_1 c_3 \hat{n}}{2\omega - \Delta_1} - \frac{\hat{n}+1}{\Delta_1}\right)\right],$$

$$\mathcal{S}_{0,2}(\hat{n}) \approx \frac{g_1 g_2}{2}\left[-\varepsilon_1^{(r)}\left(\frac{c_2 \hat{n}}{\Delta_1(2\omega - \Delta_2)} + \frac{c_1(\hat{n}+1)}{\Delta_2(2\omega - \Delta_1)}\right)\right.$$
$$\left. + \frac{\varepsilon_2^{(r)}}{2\omega - \Delta_3}\left(\frac{c_2 \hat{n}}{\Delta_1} - \frac{c_1(\hat{n}+1)}{2\omega - \Delta_1}\right)\right].$$

In this case the modulation frequency must also be adjusted according to the populated Fock state $|n\rangle$, since $\lambda_{j,n} - \lambda_{l,n} \gtrsim |\mathcal{S}_{l,j}(n)|$ for typical parameters.

At this point it is opportune to discuss the main differences between this work and the recent paper [49]. In both cases the system consisted of a nonstationary cyclic qutrit coupled to a single cavity mode, as described by the Hamiltonian (1). In Ref. [49] the goal was to find transitions that occur primarily in the cavity field, with the cyclic qutrit remaining in the *ground* state; this led to the prediction of one- and three-photon DCEs for single-tone modulations with frequencies $\eta \approx \omega$ and $\eta \approx 3\omega$, respectively. Instead, in the present paper we study single- and multitone perturbations that couple *different* atomic levels via effective multiphoton transitions, and we estimate analytically the corresponding transition rates up to four-photon effects. Additionally, here we find that in the "hybrid" regime, $\Delta_3 = 0$, the JC multiphoton transition rate increases, and multiphoton entangled states can be created from the initial state $|0, 0\rangle$ for $\eta \approx 3\omega$ (see Sec. IV). Hence, these two studies combined demonstrate the versatility of nonstationary cyclic qutrits for the engineering of sophisticated effective interactions.

We conclude this section recalling the definition of logarithmic negativity as defined in Ref. [50], which we exploit as a tool to single out the presence of entanglement in the state of the qutrit-cavity system. Given a density operator $\hat{\rho}$ of a bipartite system A-B, the logarithmic negativity is defined as

$$E_N(\rho) = \log_2 \text{tr} \sqrt{[\rho^{(A)B}]^\dagger \rho^{(A)B}},\tag{12}$$

where $\rho^{(A)B}$ is the partial transpose of $\hat{\rho}$ with respect to party A.

III. NUMERIC RESULTS

In this section we solve numerically the Schrödinger equation for the original Hamiltonian (1). To assess the experimental feasibility of the scheme we compare the unitary dynamics to the dissipative one obtained through numeric integration of the phenomenological Markovian master equation [54,56]

$$\dot{\rho} = \frac{1}{i\hbar}[\hat{H}, \hat{\rho}] + \kappa \mathcal{L}[\hat{a}] + \sum_{k=0}^{1}\sum_{l>k}^{2} \gamma_{k,l}\mathcal{L}[\hat{\sigma}_{k,l}]$$
$$+ \sum_{k=1}^{2} \gamma_k^{(\phi)}\mathcal{L}[\hat{\sigma}_{k,k}].$$

Here $\hat{\rho}$ is the density operator, $\mathcal{L}[\hat{O}] \equiv \hat{O}\hat{\rho}\hat{O}^\dagger - \hat{O}^\dagger\hat{O}\hat{\rho}/2 - \hat{\rho}\hat{O}^\dagger\hat{O}/2$ is the Lindblad superoperator, κ is the cavity relaxation rate, and $\gamma_{k,l}$ ($\gamma_k^{(\phi)}$) are the atomic relaxation (pure dephasing) rates. Notice that related works [32,46,65] demonstrated that for $g_k/\omega < 10^{-1}$ and small times this approach is a good approximation to a more rigorous microscopic model of dissipation [66].

In all the simulations we set $\varepsilon_1 = 0$ and $g_1/\omega = 0.06$. In Fig. 1 we consider the initial zero-excitation state $|0, 0\rangle$ and study the simultaneous implementation of the Hamiltonians $\hat{H}_{AJC}^{(2)}(0, 2)$ and $\hat{H}_{JC}^{(3)}(1, 2)$, adjusted to couple the states $|0, 0\rangle \rightarrow |2, 2\rangle$ and $|2, 2\rangle \rightarrow |1, 5\rangle$, respectively. We use the plausible parameters (normalized by ω): $g_2 = 0.08$, $g_3 = 0.04$, $\Delta_1 = -0.52$, $\Delta_2 = -0.54$, $\varepsilon_2 = 0.3$, $\eta^{(1)} = 5.103$
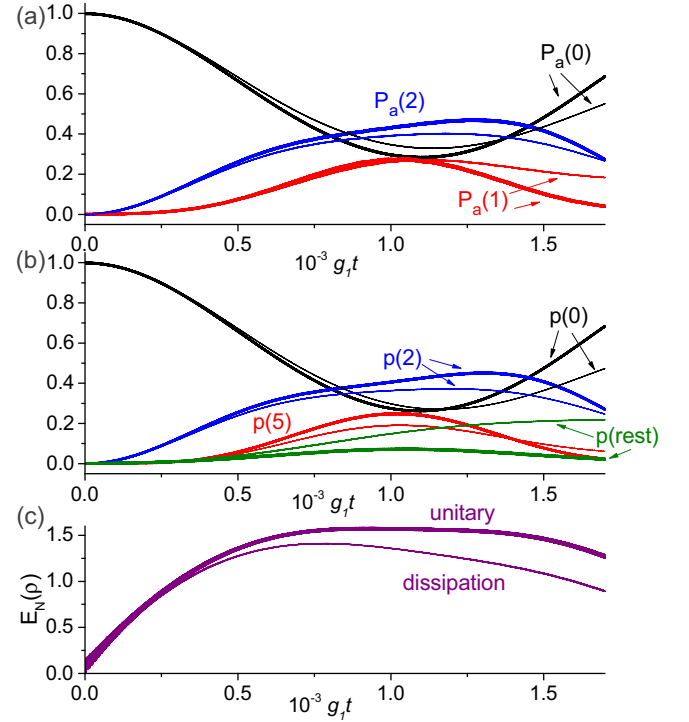

FIG. 1. Implementation of combined two-photon AJC and three-photon JC Hamiltonians for the initial state $|0, 0\rangle$. (a) Probabilities of atomic states. (b) Photon number probabilities. (c) Logarithmic negativity $E_N(\rho)$. Thick lines represent the unitary evolution and thin lines describe the evolution under Markovian dissipation. For $g_{0,1}t \sim 10^3$ one creates an entangled state composed mostly of $|0, 0\rangle$, $|1, 5\rangle$, and $|2, 2\rangle$.

(for AJC coupling), and $\eta^{(2)} = 1.398$ (for JC coupling). The weights of the modulation components are $w_2^{(1)} = 1$ and $w_2^{(2)} = 0.24$; the dissipative parameters read $\kappa = \gamma_{k,l} = 10^{-4}g_1$ and $\gamma_k^{(\phi)} = 2\kappa$. The unitary dynamics is represented by thick lines. As expected, mostly the states $|0, 0\rangle$, $|2, 2\rangle$, and $|1, 5\rangle$ are populated (with similar probabilities near the time $t_* \sim 10^3 g_1^{-1}$), and the probability of other Fock states, denoted as $p(\text{rest})$, is below 10%. In the presence of dissipation (thin lines) other states become populated, yet for $g_1t \lesssim 10^3$ the contribution of undesirable states is small. Therefore, this protocol could be implemented experimentally with present technology [59,67–74], offering an alternative manner to generate entangled qutrit-cavity states involving all the atomic levels. This fact is clearly shown through Fig. 1(c), where an increase of logarithmic negativity is visible, even in the presence of dissipation. In Fig. 2(a) we illustrate the degree of accuracy with which the effective Hamiltonian $\hat{H}_{AJC}^{(2)}(0, 2) + \hat{H}_{JC}^{(3)}(1, 2)$ describes the actual dynamics in the unitary case. As noted previously, for high-order processes our analytic results provide only the order of magnitude of the coupling parameters, so we replace $\mathcal{J}_{1,2}^{(3)} \rightarrow 0.45\mathcal{J}_{1,2}^{(3)}$ in Eq. (B1) to obtain the correct JC-coupling parameter. We see that for initial times, $g_1t \lesssim 10^3$, the agreement between the numeric results (thick lines) and the ones according to the effective Hamiltonian (thin lines) is satisfactory. For larger times the description in terms of the truncated subspace $\{|0, 0\rangle, |2, 2\rangle, |1, 5\rangle\}$ becomes clearly inadequate.
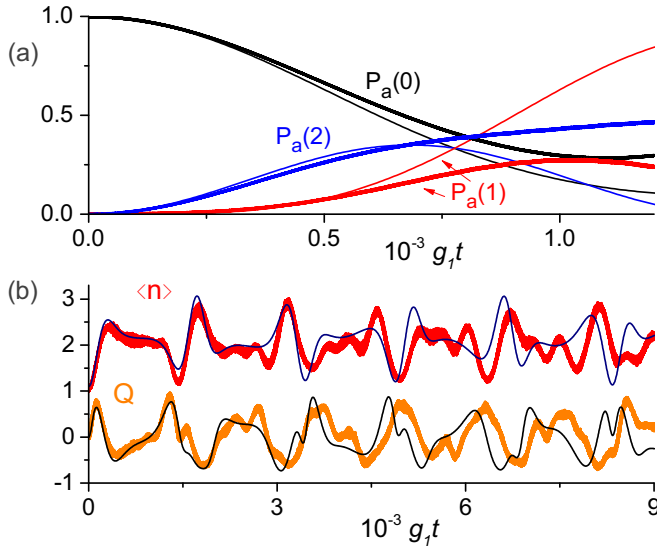
FIG. 2. Numeric results versus predictions of effective Hamiltonians. Thick lines represent the exact numeric dynamics (without dissipation), while the thin lines depict the behavior according to the effective Hamiltonians. (a) Atomic populations corresponding to Fig. 1(a) (initial state $|\mathbf{0}, 0\rangle$). (b) Average photon number and Mandel's factor corresponding to Fig. 3(a) (initial state $|\mathbf{0}\rangle \otimes |\alpha\rangle$). For initial times, the simplified analytic description in terms of effective Hamiltonians approximates satisfactorily the exact dynamics. This is remarkable, since the effective Hamiltonians neglect the dressing of the bare states $|\mathbf{k}, n\rangle$ and all the off-resonant transitions.

In Fig. 3 we choose the regime of parameters for which $\hat{H}_{\text{AJC}}^{(2)}(0, 1)$ can couple several states $|\mathbf{0}, k\rangle \leftrightarrow |\mathbf{1}, k + 2\rangle$ for $0 \leqslant k \lesssim 4$: $g_2 = 1.03 g_1$, $g_3 = 0.38 g_1$, $\Delta_1 = 7.5 g_1$, $\Delta_2 = 5.83 g_1$, $\varepsilon_2 = 0.12 \omega$, $\eta = 2.548 \omega$, $\kappa = 5 \times 10^{-5} g_1$, and $\gamma_{k,l} = \gamma_k^{(\phi)} = \kappa/2$. We consider the initial state $|\mathbf{0}\rangle \otimes |\alpha\rangle$, where $|\alpha\rangle$ is the coherent state with the average photon number $\alpha^2 = 1.1$. Figure 3(c) proves that indeed several Fock states are coupled by the single-tone modulation (for the sake of clarity we omitted the corresponding results in the presence of dissipation), giving rise to nonperiodic oscillation of the average photon number $\langle n \rangle$, atomic population $P_a(1)$, and the Mandel's factor $Q = [\langle (\Delta n)^2 \rangle - \langle n \rangle] / \langle n \rangle$. As expected, the population of the atomic level $|\mathbf{2}\rangle$ remains nearly zero, undergoing fast oscillations due to off-resonant couplings. Moreover, for the assumed low dissipative rates, the time evolution is virtually unaffected by dissipation for $g_1 t \lesssim 10^3$. Hence Fig. 3 confirms that one can emulate effective Hamiltonians that couple multiple pairs of states by properly choosing the system parameters and the modulation frequency. In Fig. 2(b) we compare the results of Fig. 3(a) to the dynamics according to the effective Hamiltonian $\hat{H}_{\text{AJC}}^{(2)}(0, 1)$ with the coupling strength (11). Again, the agreement is quite good for initial times, $g_1 t \lesssim 10^3$; for larger times the deviations occur mainly because the modulation frequency goes off resonance for Fock states with $k \gtrsim 4$.

In Fig. 4 we illustrate the implementation of the four-photon JC Hamiltonian $\hat{H}_{\text{JC}}^{(4)}(0, 1)$ for the initial state $|\mathbf{1}, 0\rangle$ and the following parameters (normalized by ω): $g_2 = 0.08$, $g_3 = 0.04$, $\Delta_1 = -0.66$, $\Delta_2 = 0.42$, $\eta = 2.301$, $\varepsilon_2 =$
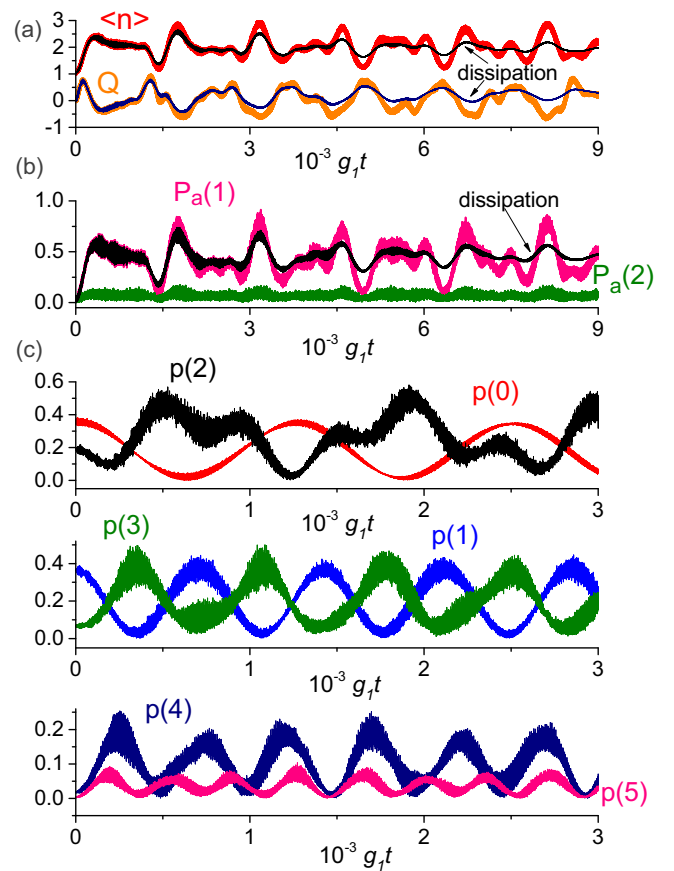

FIG. 3. Effective two-photon AJC model for the initial coherent state $|\mathbf{0}\rangle \otimes |\alpha\rangle$. (a) Time evolution of the average photon number $\langle n \rangle$ and the Mandel's Q factor under unitary (thick lines) and lossy (thin lines) evolutions. (b) Atomic populations. (c) Photon-number probabilities during unitary evolution. In this regime of parameters a single-tone modulation couples several doublets $|\mathbf{0}, k\rangle \leftrightarrow |\mathbf{1}, k + 2\rangle$ with transition rates $\propto \sqrt{(k + 1)(k + 2)}$.

0.22, and $\gamma_{k,l} = \gamma_k^{(\phi)} = \kappa = 5 \times 10^{-5} g_1$. The exact numeric dynamics (thick lines) resembles quite well the expected four-photon exchange, though the analytical transition rate, Eq. (B2), overestimates the actual rate by a factor of 2 (data not shown). Since in reality the modulation induces coupling between the dressed states $|\beta_{1,0}\rangle$ and $|\beta_{0,4}\rangle$, it is not surprising that in the unitary case the (small) population $p(3)$ oscillates with the same period as $p(4)$. The population of the atomic level $P_a(2)$ is always less than 2%, so it is not shown. In our scheme, the higher-order Hamiltonians naturally have smaller transition rates due to the multiplicative factors g_i/Δ_k and g_i/ω. As shown by thin lines in Fig. 4, in this case even very weak dissipation suffices to inhibit the oscillatory behavior. Fortunately, for *n*-photon JC models we can surpass this limitation by exploring the "hybrid transitions" described in the next section.

IV. HYBRID TRANSITIONS FOR $\Delta_3 = 0$

We can speed up the *n*-photon JC transitions between the atomic states $|\mathbf{0}\rangle$ and $|\mathbf{1}\rangle$ by setting $\Delta_2 = -\Delta_1$, maintaining $|\Delta_1| \gg g_k \sqrt{n_{\max}}$. In this case, the dominant part of the bare
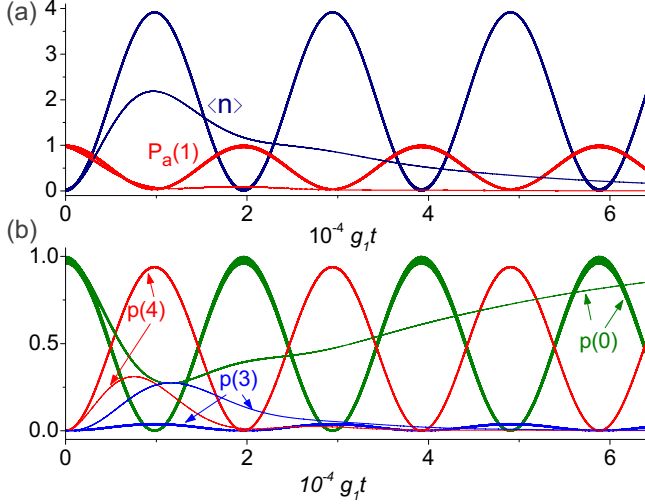
FIG. 4. Approximate implementation of the four-photon JC Hamiltonian for the initial state $|1, 0\rangle$. (a) Average photon number and the atomic population. (b) Relevant photon number probabilities. Thick (thin) lines represent the unitary (dissipative) evolution. In the lossless case, the main transition is between the states $|1, 0\rangle \leftrightarrow |0, 4\rangle$, but other states also become slightly populated due to their presence in the dressed states, Eqs. (7) and (8), as illustrated by $p(3)$.

Hamiltonian is $\hat{H}_{\mathrm{aux}} \equiv \hat{H}_0[c_1 = c_2 = g_3 = 0]$, with the m-excitation eigenfrequencies and eigenstates (see Ref. [48] for exact expressions): $|\xi_0\rangle = |0, 0\rangle$, $\lambda_0^{(0)} = 0$, and for $m \geqslant 1$

$$\lambda_{m,-}^{(0)} \approx m\omega - \Delta_1 - \left(K_m^2/\Delta_1 - K_m^4/\Delta_1^3\right),$$

$$\lambda_{m \geqslant 2, 0}^{(0)} = m\omega,$$

$$\lambda_{m,+}^{(0)} \approx m\omega + \left(K_m^2/\Delta_1 - K_m^4/\Delta_1^3\right), \quad (13)$$

$$|\xi_{m,-}\rangle \approx \left(1 - \frac{3K_m^2}{2\Delta_1^2}\right) \frac{g_1\sqrt{m}|0, m\rangle + g_2\sqrt{m-1}|2, m-2\rangle}{\Delta_1}$$
$$- \left(1 - \frac{K_m^2}{2\Delta_1^2}\right)|1, m-1\rangle,$$

$$|\xi_{m \geqslant 2, 0}\rangle = \frac{g_2\sqrt{m-1}|0, m\rangle - g_1\sqrt{m}|2, m-2\rangle}{K_m},$$

$$|\xi_{m,+}\rangle \approx \left(1 - \frac{K_m^2}{2\Delta_1^2}\right) \frac{g_1\sqrt{m}|0, m\rangle + g_2\sqrt{m-1}|2, m-2\rangle}{K_m}$$
$$+ \frac{K_m}{\Delta_1}\left(1 - \frac{3K_m^2}{2\Delta_1^2}\right)|1, m-1\rangle, \quad (14)$$

where $K_m \equiv \sqrt{mg_1^2 + (m-1)g_2^2}$. For $g_1 \sim g_2$ one can crudely picture these dressed states as $|\xi_{m,-}\rangle \sim |1, m-1\rangle$, $|\xi_{m \geqslant 2, 0}\rangle \sim (|0, m\rangle - |2, m-2\rangle)/\sqrt{2}$, and $|\xi_{m \geqslant 2, +}\rangle \sim (|0, m\rangle + |2, m-2\rangle)/\sqrt{2}$.

The complete dressed states $|\varphi_{m,s}\rangle$ can be obtained in a straightforward manner from the perturbation theory with the perturbation $\hat{V} = \hat{H}_0 - \hat{H}_{\mathrm{aux}}$. One immediately sees that the first-order energy shifts $\hbar\lambda_{m,s}^{(1)} = \langle\xi_{m,s}|\hat{V}|\xi_{m,s}\rangle$ are zero because $\hat{V}$ does not conserve the total number of excitations.

Hence the correction to the eigenfrequencies, Eqs. (13) and (14), will be $\sim O(g^2/\omega)$ (where g stands for the order of magnitude of g_k); for example, for the ground state one obtains $\lambda_0^{(2)} \approx -[c_1g_1^2/(2\omega - \Delta_1) + c_3g_3^2/3\omega]$. To evaluate the transition rates $\Theta_{m;n}^{(j)}$ in Eq. (3) we need the first-order corrections to the eigenstates. For example, for the ground state one gets

$$|\xi_0^{(1)}\rangle \approx \frac{c_1g_1}{2\omega - \Delta_1}|\xi_{2,-}\rangle - \frac{c_1g_1K_2}{2\omega\Delta_1}|\xi_{2,+}\rangle + \frac{\sqrt{3}c_3g_1g_3}{3\omega K_3}|\xi_{3,0}\rangle$$
$$- \frac{\sqrt{2}c_3g_2g_3}{\Delta_1(3\omega - \Delta_1)}|\xi_{3,-}\rangle - \frac{\sqrt{2}c_3g_2g_3}{3\omega K_3}|\xi_{3,+}\rangle.$$

The expressions for other states are calculated analogously, but for the sake of space we omit them here.

One can achieve the JC-like transitions by employing the hybrid states $|\varphi_{m \geqslant 2, 0}\rangle$ and $|\varphi_{m \geqslant 2, +}\rangle$, which contain approximately equal contributions of the atomic states $|0\rangle$ and $|2\rangle$ and lack the state $|1\rangle$. For instance, the three-excitation transitions between the states $|\varphi_{m,-}\rangle \leftrightarrow |\varphi_{m+3,+}\rangle$ and $|\varphi_{m,-}\rangle \leftrightarrow |\varphi_{m+3,0}\rangle$ have the transition rates

$$\frac{\Theta_{m,-;m+3,+}^{(j)}}{\sqrt{m(m+1)(m+2)}} = -\frac{c_3g_1g_2g_3}{2K_{m+3}(3\omega + \Delta_1)}\left[\frac{\varepsilon_1^{(j)}}{3\omega} + \frac{\varepsilon_2^{(j)}}{\Delta_1}\right],$$

$$\frac{\Theta_{m,-;m+3,0}^{(j)}}{\sqrt{m(m+1)(m+3)}} = \frac{c_3g_1^2g_3}{2K_{m+3}(3\omega + \Delta_1)}\left[\frac{\varepsilon_1^{(j)}}{3\omega} + \frac{\varepsilon_2^{(j)}}{\Delta_1}\right].$$

For the typical scenario $g_2 > g_1$ [53], by choosing the modulation frequency $\eta = \lambda_{m+3,0} - \lambda_{m,-}$, one can achieve the four-photon JC transition $|1, m\rangle \leftrightarrow |0, m+4\rangle$, with the transition rate at least 1 order of magnitude larger than in the previous section [cf. Eq. (B2)]. However, the price for such an impressive speed-up is the simultaneous excitation of the state $|2, m+2\rangle$, whose probability is $\sim(g_2/g_1)^2$ times smaller than the probability of the state $|0, m+4\rangle$. As an example, in Fig. 5 we consider the initial state $|1, 0\rangle$ and the same parameters as in Fig. 4 except for $\varepsilon_2 = 0.2\omega$, $\eta = 2.289\omega$, and $\Delta_2 = -\Delta_1$. As expected, the transition rate is roughly ten times larger than in Fig. 4, so this effect is robust against moderate dissipation. Mostly the states $|1, 0\rangle$ and $|0, 4\rangle$ are populated; the population of the state $|2, 2\rangle$ is expected from the dressed state $|\xi_{4,0}\rangle$, and the small probability of three photons (in the unitary case) arises from other nonresonant transitions in Eq. (3).

The regime $\Delta_3 = 0$ is also attractive to generate entangled states with multiple excitations from the initial zero-excitation state. One possibility is the transition $|\varphi_0\rangle \leftrightarrow |\varphi_{3,+}\rangle$ when $\eta \approx \lambda_{3,+}$, for which

$$\Theta_{0;3,+}^{(j)} = \frac{c_3g_2g_3}{3\sqrt{2}K_3\omega}\left[\frac{K_3^2}{\Delta_1(3\omega - \Delta_1)}\varepsilon_1^{(j)} - \varepsilon_2^{(j)}\right].$$

However, only three excitations can be generated in this case because the resonant modulation frequency goes off resonance by $\sim g_1^2/\Delta_1$ as the number of excitations increases [see Eq. (14)]. On the other hand, since $\lambda_{m+3,0} - \lambda_{m,0} = 3\omega + O(g_k^2/\omega)$, for $\eta \approx 3\omega$ one expects the generation of a larger number of photons due to the simultaneous nearly resonant transitions $|\varphi_0\rangle \leftrightarrow |\varphi_{3,0}\rangle \leftrightarrow |\varphi_{6,0}\rangle \leftrightarrow \cdots$. Notice that this effect takes place only for cyclic qutrits (as do the
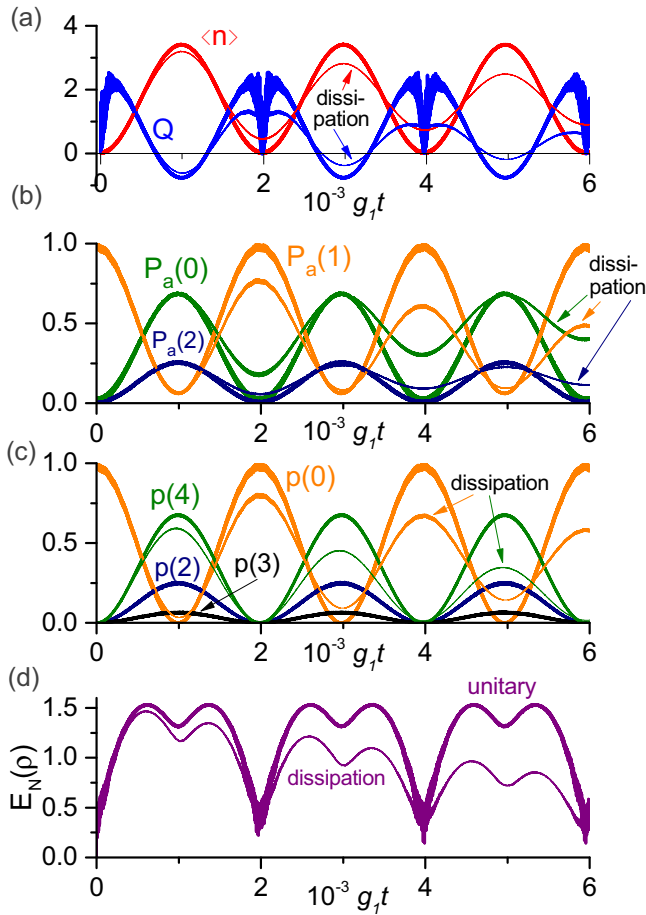
FIG. 5. Four-photon JC-like transition to the hybrid state $|\varphi_{4,0}\rangle$. Unitary (thick lines) and dissipative (thin lines) dynamics are shown for the initial state $|\mathbf{1}, 0\rangle$. (a) Average photon number and the Mandel's factor. (b) Atomic populations. (c) Photon number probabilities [the probabilities $p(3)$ and $p(4)$ in the presence of dissipation are omitted for the sake of clarity]. (d) Logarithmic negativity.

FIG. 6. Generation of multiphoton entangled states via hybrid transitions for the initial state $|\mathbf{0}, 0\rangle$ and the modulation frequency $\eta \approx 3\omega$ (without dissipation). (a) Average photon number (thick line) and the Mandel's factor (thin line). (b) Atomic populations. (c) Relevant photon number probabilities and the logarithmic negativity.

one- and three-photon DCEs described in Ref. [49]), since the associated transition rate reads

$$\Theta^{(j)}_{m,0;m+3,0} = \frac{c_3 g_1 g_2 g_3}{6\omega K_m K_{m+3}} \varepsilon_2^{(j)} \sqrt{(m-1)(m+1)(m+3)}$$

(this expression remains formally valid for $m = 0$). In Fig. 6 we illustrate the typical unitary dynamics for the parameters of Fig. 5 except for $\eta = 3.004\omega$. We see that the atomic level $|\mathbf{1}\rangle$ remains nearly unpopulated, while the average photon number oscillates between 0 and 5. The timescale of this effect is comparable to the one of the two-photon AJC transition illustrated in Fig. 1. Moreover, the Q factor becomes negative when $\langle n \rangle$ attains its local maxima, indicating a generation of nonclassical field states. In Fig. 6(c) we also plot the largest photon number probabilities $p(n)$, demonstrating that Fock states with up to ten photons become populated. Concerning the entanglement generation, we observe that both in Figs. 5(d) and 6(c) logarithmic negativity is mainly above unity, with the exception of those regions where the mean photon number approaches zero or an atomic population approaches unity,
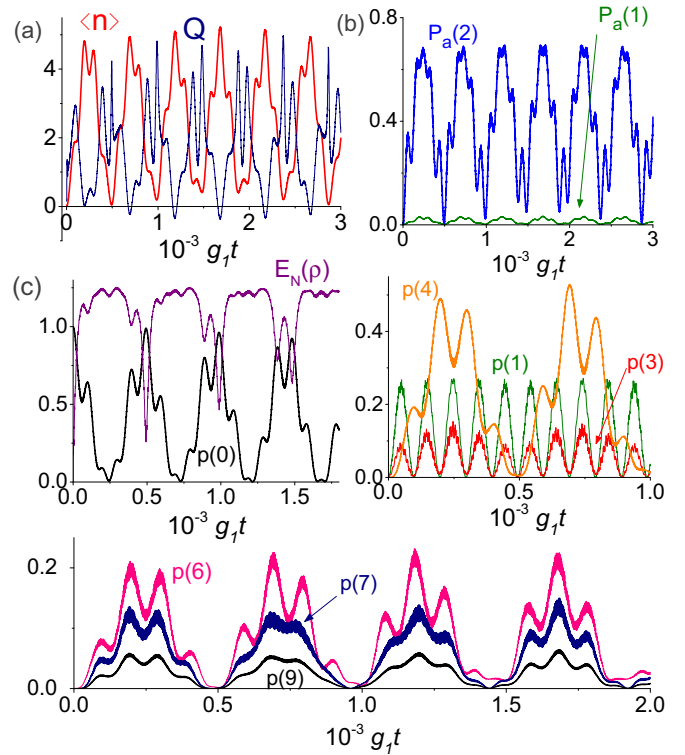
since each of such conditions implies that the qutrit-cavity state is almost factorized. In Fig. 5(d) the detrimental effect of dissipation is clearly visible, though entanglement production remains possible even for a relatively long time.

V. CONCLUSIONS

It was shown analytically and numerically that coupling a single cavity mode with a qutrit in the cyclic configuration can represent a good starting point to realize dynamics that emulate the ones stemming from the JC and AJC models. We have proved the possibility of realizing effective *n*-photon JC or AJC evolutions, as well as a combined dynamics, by appropriately modulating the qutrit energy levels in the dispersive regime. To assess the experimental feasibility of our proposal we have also considered the presence of Markovian noise, showing a certain level of robustness against environment-induced fluctuations. Some limitations deriving from the lowering of the transition rates for high-order JC models can be overcome by exploring the hybrid transitions in the regime $\Delta_1 = -\Delta_2$, when the JC transition rate increases substantially at the expense of generating an entangled atom-cavity state. Finally, we have shown that this feature allows for a straightforward way of generating entangled states with multiple excitations starting from the zero-excitation state.

APPENDIX A: PERTURBATIVE CORRECTIONS

The second-order corrections to the eigenstates are

$$
\begin{aligned}
|\mathbf{0},k\rangle_{(2)} ={}& \frac{\sqrt{(k+1)(k+2)}}{2\omega}\left[\frac{c_1 g_1^2}{2\omega-\Delta_1}+\frac{c_3 g_3^2}{3\omega-\Delta_3}\right]|\mathbf{0},k+2\rangle + \frac{\sqrt{k(k-1)}}{2\omega}\left[\frac{c_1 g_1^2}{\Delta_1}-\frac{c_3 g_3^2}{\omega-\Delta_3}\right]|\mathbf{0},k-2\rangle \\
&+\frac{c_3 g_2 g_3\sqrt{(k+1)(k+2)}}{(3\omega-\Delta_3)(3\omega-\Delta_1)}|\mathbf{1},k+2\rangle+\frac{g_2 g_3}{\omega-\Delta_1}\left[\frac{k}{\omega-\Delta_3}+\frac{c_2 c_3(k+1)}{3\omega-\Delta_3}\right]|\mathbf{1},k\rangle-\frac{c_2 g_2 g_3\sqrt{k(k-1)}}{(\omega-\Delta_3)(\omega+\Delta_1)}|\mathbf{1},k-2\rangle \\
&+\frac{c_1 c_2 g_1 g_2\sqrt{(k+1)(k+2)}}{(2\omega-\Delta_1)(4\omega-\Delta_3)}|\mathbf{2},k+2\rangle+\frac{g_1 g_2}{2\omega-\Delta_3}\left[\frac{c_1(k+1)}{2\omega-\Delta_1}-\frac{c_2 k}{\Delta_1}\right]|\mathbf{2},k\rangle+\frac{g_1 g_2\sqrt{k(k-1)}}{\Delta_1\Delta_3}|\mathbf{2},k-2\rangle,
\end{aligned}
$$

$$
\begin{aligned}
|\mathbf{1},k\rangle_{(2)} ={}& \frac{c_2 g_2 g_3\sqrt{(k+1)(k+2)}}{(2\omega-\Delta_2)(\omega+\Delta_1)}|\mathbf{0},k+2\rangle+\frac{g_2 g_3}{\omega-\Delta_1}\left(\frac{k}{\Delta_2}-\frac{c_2 c_3(k+1)}{2\omega-\Delta_2}\right)|\mathbf{0},k\rangle+\frac{c_3 g_2 g_3\sqrt{k(k-1)}}{\Delta_2(3\omega-\Delta_1)}|\mathbf{0},k-2\rangle \\
&+\frac{\sqrt{(k+1)(k+2)}}{2\omega}\left(\frac{c_1 g_1^2}{\Delta_1}+\frac{c_2 g_2^2}{2\omega-\Delta_2}\right)|\mathbf{1},k+2\rangle+\frac{\sqrt{k(k-1)}}{2\omega}\left(\frac{c_1 g_1^2}{2\omega-\Delta_1}+\frac{c_2 g_2^2}{\Delta_2}\right)|\mathbf{1},k-2\rangle \\
&+\frac{c_3 g_1 g_3\sqrt{(k+1)(k+2)}}{\Delta_1(3\omega-\Delta_2)}|\mathbf{2},k+2\rangle+\frac{g_1 g_3}{\omega-\Delta_2}\left(\frac{k+1}{\Delta_1}-\frac{c_1 c_3 k}{2\omega-\Delta_1}\right)|\mathbf{2},k\rangle+\frac{c_1 g_1 g_3\sqrt{k(k-1)}}{(2\omega-\Delta_1)(\omega+\Delta_2)}|\mathbf{2},k-2\rangle,
\end{aligned}
$$

$$
\begin{aligned}
|\mathbf{2},k\rangle_{(2)} ={}& \frac{g_1 g_2\sqrt{(k+1)(k+2)}}{\Delta_2\Delta_3}|\mathbf{0},k+2\rangle+\frac{g_1 g_2}{2\omega-\Delta_3}\left(\frac{c_2 k}{2\omega-\Delta_2}-\frac{c_1(k+1)}{\Delta_2}\right)|\mathbf{0},k\rangle+\frac{c_1 c_2 g_1 g_2\sqrt{k(k-1)}}{(2\omega-\Delta_2)(4\omega-\Delta_3)}|\mathbf{0},k-2\rangle \\
&-\frac{c_1 g_1 g_3\sqrt{(k+1)(k+2)}}{(\omega-\Delta_3)(\omega+\Delta_2)}|\mathbf{1},k+2\rangle+\frac{g_1 g_3}{\omega-\Delta_2}\left(\frac{k+1}{\omega-\Delta_3}+\frac{c_1 c_3 k}{3\omega-\Delta_3}\right)|\mathbf{1},k\rangle+\frac{c_3 g_1 g_3\sqrt{k(k-1)}}{(3\omega-\Delta_3)(3\omega-\Delta_2)}|\mathbf{1},k-2\rangle \\
&+\frac{\sqrt{(k+1)(k+2)}}{2\omega}\left(\frac{c_2 g_2^2}{\Delta_2}-\frac{c_3 g_3^2}{\omega-\Delta_3}\right)|\mathbf{2},k+2\rangle+\frac{\sqrt{k(k-1)}}{2\omega}\left(\frac{c_2 g_2^2}{2\omega-\Delta_2}+\frac{c_3 g_3^2}{3\omega-\Delta_3}\right)|\mathbf{2},k-2\rangle.
\end{aligned}
$$

The third- and fourth-order corrections are obtained analogously, but we omit the explicit expressions here.

The fourth-order corrections to the eigenfrequencies read

$$
\begin{aligned}
\lambda_{0,k}^{(4)} ={}& \frac{k g_1^2}{\Delta_1}\left\{\frac{c_1(k-1)}{2\omega}\left[\frac{g_1^2}{\Delta_1}-\frac{c_3 g_3^2}{\omega-\Delta_3}\right]+\frac{c_2 g_2^2}{2\omega-\Delta_3}\left[\frac{c_1(k+1)}{2\omega-\Delta_1}-\frac{k}{\Delta_1}\right]+\frac{g_2^2(k-1)}{\Delta_1\Delta_3}-\frac{\lambda_{0,k}^{(2)}}{\Delta_1}\right\} \\
&-\frac{c_1 g_1^2(k+1)}{2\omega-\Delta_1}\left\{\frac{k+2}{2\omega}\left[\frac{g_1^2}{2\omega-\Delta_1}+\frac{c_3 g_3^2}{3\omega-\Delta_3}\right]+\frac{g_2^2}{2\omega-\Delta_3}\left[\frac{k+1}{2\omega-\Delta_1}-\frac{c_2 k}{\Delta_1}\right]+\frac{c_2 g_2^2(k+2)}{(4\omega-\Delta_3)(2\omega-\Delta_1)}+\frac{\lambda_{0,k}^{(2)}}{2\omega-\Delta_1}\right\} \\
&+\frac{g_3^2 k}{\omega-\Delta_3}\left\{\frac{c_2 g_2^2(k-1)}{(\omega-\Delta_3)(\omega+\Delta_1)}-\frac{g_2^2}{\omega-\Delta_1}\left[\frac{k}{\omega-\Delta_3}+\frac{c_2 c_3(k+1)}{3\omega-\Delta_3}\right]-\frac{c_3(k-1)}{2\omega}\left[\frac{c_1 g_1^2}{\Delta_1}-\frac{g_3^2}{\omega-\Delta_3}\right]-\frac{\lambda_{0,k}^{(2)}}{\omega-\Delta_3}\right\} \\
&-\frac{c_3 g_3^2(k+1)}{3\omega-\Delta_3}\left\{\frac{\frac{g_2^2(k+2)}{3\omega-\Delta_1}+\lambda_{0,k}^{(2)}}{3\omega-\Delta_3}+\frac{c_2 g_2^2}{\omega-\Delta_1}\left[\frac{k}{\omega-\Delta_3}+\frac{c_2(k+1)}{3\omega-\Delta_3}\right]+\frac{k+2}{2\omega}\left[\frac{c_1 g_1^2}{2\omega-\Delta_1}+\frac{g_3^2}{3\omega-\Delta_3}\right]\right\},
\end{aligned}
$$

$$
\begin{aligned}
\lambda_{1,k}^{(4)} ={}& -\frac{g_1^2(k+1)}{\Delta_1}\left\{\frac{c_1(k+2)}{2\omega}\left[\frac{g_1^2}{\Delta_1}+\frac{g_2^2 c_2}{2\omega-\Delta_2}\right]+\frac{g_3^2\left(\frac{k+1}{\Delta_1}-\frac{c_1 c_3 k}{2\omega-\Delta_1}\right)}{\omega-\Delta_2}+\frac{c_3 g_3^2(k+2)}{\Delta_1(3\omega-\Delta_2)}+\frac{\lambda_{1,k}^{(2)}}{\Delta_1}\right\} \\
&+\frac{c_1 g_1^2 k}{2\omega-\Delta_1}\left\{\frac{(k-1)\left(\frac{g_1^2}{2\omega-\Delta_1}+\frac{c_2 g_2^2}{\Delta_2}\right)}{2\omega}+\frac{g_3^2(k-1)}{(\omega+\Delta_2)(2\omega-\Delta_1)}+\frac{c_3 g_3^2\left(\frac{k+1}{\Delta_1}-\frac{k}{2\omega-\Delta_1}\right)}{\omega-\Delta_2}-\frac{\lambda_{1,k}^{(2)}}{2\omega-\Delta_1}\right\}
\end{aligned}
$$

$$+ \frac{g_2^2 k}{\Delta_2} \left\{ \frac{c_2(k-1)}{2\omega} \left[\frac{c_1 g_1^2}{2\omega - \Delta_1} + \frac{g_2^2}{\Delta_2} \right] + \frac{g_3^2}{\omega - \Delta_1} \left[\frac{k}{\Delta_2} - \frac{c_2 c_3(k+1)}{2\omega - \Delta_2} \right] + \frac{c_3 g_3^2(k-1)}{\Delta_2(3\omega - \Delta_1)} - \frac{\lambda_{1,k}^{(2)}}{\Delta_2} \right\}$$

$$- \frac{c_2 g_2^2(k+1)}{2\omega - \Delta_2} \left\{ \frac{(k+2)\left(\frac{c_1 g_1^2}{\Delta_1} + \frac{g_2^2}{2\omega - \Delta_2}\right)}{2\omega} + \frac{g_3^2(k+2)}{(2\omega - \Delta_2)(\omega + \Delta_1)} + \frac{c_3 g_3^2\left(\frac{k}{\Delta_2} - \frac{k+1}{2\omega - \Delta_2}\right)}{\omega - \Delta_1} + \frac{\lambda_{1,k}^{(2)}}{2\omega - \Delta_2} \right\},$$

$$\lambda_{2,k}^{(4)} = - \frac{g_2^2(k+1)}{\Delta_2} \left\{ \frac{g_1^2(k+2)}{\Delta_2 \Delta_3} + \frac{c_1 g_1^2}{2\omega - \Delta_3} \left[\frac{c_2 k}{2\omega - \Delta_2} - \frac{k+1}{\Delta_2} \right] + \frac{c_2(k+2)}{2\omega} \left[\frac{g_2^2}{\Delta_2} - \frac{c_3 g_3^2}{\omega - \Delta_3} \right] + \frac{\lambda_{2,k}^{(2)}}{\Delta_2} \right\}$$

$$+ \frac{c_2 g_2^2 k}{2\omega - \Delta_2} \left\{ \frac{g_1^2\left(\frac{k}{2\omega - \Delta_2} - \frac{c_1(k+1)}{\Delta_2}\right)}{2\omega - \Delta_3} + \frac{c_1 g_1^2(k-1)}{(4\omega - \Delta_3)(2\omega - \Delta_2)} + \frac{(k-1)\left(\frac{g_2^2}{2\omega - \Delta_2} + \frac{g_3^2 c_3}{3\omega - \Delta_3}\right)}{2\omega} - \frac{\lambda_{2,k}^{(2)}}{2\omega - \Delta_2} \right\}$$

$$+ \frac{g_3^2(k+1)}{\omega - \Delta_3} \left\{ \frac{g_1^2\left(\frac{k+1}{\omega - \Delta_3} + \frac{c_1 c_3 k}{3\omega - \Delta_3}\right)}{\omega - \Delta_2} - \frac{c_1 g_1^2(k+2)}{(\omega + \Delta_2)(\omega - \Delta_3)} + \frac{c_3(k+2)}{2\omega} \left(\frac{c_2 g_2^2}{\Delta_2} - \frac{c_3 g_3^2}{\omega - \Delta_3} \right) - \frac{\lambda_{2,k}^{(2)}}{\omega - \Delta_3} \right\}$$

$$+ \frac{c_3 g_3^2 k}{3\omega - \Delta_3} \left\{ \frac{g_1^2(k-1)}{(3\omega - \Delta_2)(3\omega - \Delta_3)} + \frac{c_1 g_1^2\left(\frac{k+1}{\omega - \Delta_3} + \frac{c_1 k}{3\omega - \Delta_3}\right)}{\omega - \Delta_2} + \frac{(k-1)\left(\frac{c_2 g_2^2}{2\omega - \Delta_2} + \frac{g_3^2}{3\omega - \Delta_3}\right)}{2\omega} - \frac{\lambda_{2,k}^{(2)}}{3\omega - \Delta_3} \right\},$$

where $\lambda_{n,k}^{(2)}$ are the second-order corrections from Eqs. (4)–(6).

APPENDIX B: APPROXIMATE EXPRESSIONS FOR THREE- AND FOUR-PHOTON MODELS

(i) Three-photon models:

$$\mathcal{J}_{0,1}^{(3)} \approx \frac{g_1}{2\omega} \left[\frac{\varepsilon_1^{(r)}}{2} \left(\frac{c_1 g_1^2}{\Delta_1^2} + \frac{c_2 g_2^2}{\Delta_1 \Delta_3} - \frac{c_3 g_3^2}{2\omega^2} \right) - \frac{\varepsilon_2^{(r)}}{\Delta_1} \left(\frac{c_2 g_2^2}{2\Delta_3} + \frac{c_3 g_3^2}{3\omega} \right) \right],$$

$$\mathcal{A}_{0,1}^{(3)} \approx \frac{c_1 g_1}{4\omega^2} \left[\frac{\varepsilon_1^{(r)}}{2} \left(\frac{3 c_1 g_1^2}{4\omega} + \frac{c_2 g_2^2}{\Delta_2} + \frac{c_3 g_3^2}{6\omega} \right) - \varepsilon_2^{(r)} \left(\frac{c_2 g_2^2}{4\Delta_2} - \frac{c_3 g_3^2}{3\omega} \right) \right],$$

$$\mathcal{J}_{1,2}^{(3)} \approx \frac{g_2}{2\omega} \left[\varepsilon_2^{(r)} \left(\frac{c_1 g_1^2}{8\omega^2} + \frac{c_2 g_2^2}{2\Delta_2^2} - \frac{c_3 g_3^2}{3\omega \Delta_2} \right) - \frac{\varepsilon_1^{(r)}}{2} \left(\frac{c_1 g_1^2}{\Delta_2 \Delta_3} + \frac{c_2 g_2^2}{\Delta_2^2} - \frac{c_3 g_3^2}{2\omega^2} \right) \right],$$

$$\mathcal{A}_{1,2}^{(3)} \approx \frac{c_2 g_2}{8\omega^2} \left[\frac{\varepsilon_2^{(r)}}{2} \left(\frac{c_1 g_1^2}{\Delta_1} + \frac{3 c_2 g_2^2}{2\omega} + \frac{5 c_3 g_3^2}{3\omega} \right) - \varepsilon_1^{(r)} \left(\frac{c_1 g_1^2}{\Delta_1} + \frac{3 c_2 g_2^2}{4\omega} + \frac{c_3 g_3^2}{6\omega} \right) \right],$$

$$\mathcal{J}_{0,2}^{(3)} \approx \frac{g_3}{2\omega^2} \left[\varepsilon_1^{(r)} \left(-\frac{c_1 g_1^2}{\Delta_1} + \frac{c_2 g_2^2}{\Delta_2} \right) + \varepsilon_2^{(r)} \left(\frac{c_1 g_1^2}{2\Delta_1} - \frac{c_2 g_2^2}{2\Delta_2} + \frac{c_3 g_3^2 \Delta_3}{\omega^2} \right) \right],$$

$$\mathcal{A}_{0,2}^{(3)} \approx \frac{c_3 g_3}{40\omega^3} \left[\varepsilon_1^{(r)} \left(c_1 g_1^2 - c_2 g_2^2 \right) + \varepsilon_2^{(r)} \left(c_1 g_1^2 + 2 c_2 g_2^2 + 2 c_3 g_3^2 \right) \right]. \tag{B1}$$

(ii) Four-photon models:

$$\mathcal{J}_{0,1}^{(4)} \approx \frac{g_2 g_3}{2\omega} \left\{ \varepsilon_2^{(r)} \left[\frac{g_1^2}{\Delta_1} \left(\frac{c_3}{3\Delta_1 \Delta_3} - \frac{c_1 c_2}{8\omega^2} \right) + \frac{c_2 g_2^2}{2\omega^3} + \frac{3 c_2 c_3 g_3^2}{8\omega^3} \right] - \frac{\varepsilon_1^{(r)}}{\omega} \left[\frac{g_1^2}{\Delta_1} \left(\frac{c_3 \Delta_2}{9\Delta_1 \Delta_3} + \frac{c_1 c_2}{2\omega} \right) + \frac{c_2 g_2^2}{2\omega^2} + \frac{c_2 c_3 g_3^2}{6\omega^2} \right] \right\},$$

$$\mathcal{A}_{0,1}^{(4)} \approx \frac{g_2 g_3}{2\omega^3} \left\{ \varepsilon_1^{(r)} \left[\frac{c_1 g_1^2}{6} \left(\frac{c_3}{3\Delta_2} + \frac{c_2}{2\omega} \right) - \frac{c_2 c_3 g_2^2}{18\Delta_2} - \frac{c_3 g_3^2}{150\omega} \right] - \frac{\varepsilon_2^{(r)}}{4} \left[c_1 g_1^2 \left(\frac{c_2}{4\omega} - \frac{c_3}{5\Delta_2} \right) - \frac{c_2 c_3 g_2^2}{3\Delta_2} - \frac{c_3 g_3^2}{3\Delta_2} \right] \right\},$$

$$\mathcal{J}_{1,2}^{(4)} \approx \frac{g_1 g_3}{2\omega} \left\{ \varepsilon_2^{(r)} \left[\frac{c_1 g_1^2}{48\omega^3} + \frac{g_2^2}{\Delta_2} \left(\frac{3 c_1 c_2}{5\omega^2} - \frac{c_3}{3\Delta_2 \Delta_3} \right) - \frac{c_1 c_3 g_3^2}{4\omega^3} \right] - \frac{\varepsilon_1^{(r)}}{\omega} \left[\frac{c_1 g_1^2}{2\omega^2} + \frac{g_2^2}{\Delta_2} \left(\frac{c_1 c_2}{2\omega} + \frac{c_3 \Delta_1}{9\Delta_2 \Delta_3} \right) + \frac{c_1 c_3 g_3^2}{6\omega^2} \right] \right\},$$

$$\mathcal{A}_{1,2}^{(4)} \approx - \frac{g_1 g_3}{2\omega^3} \left\{ \frac{\varepsilon_1^{(r)}}{6} \left[\frac{c_1 c_3 g_1^2}{3\Delta_1} - c_2 g_2^2 \left(\frac{c_3}{3\Delta_1} + \frac{c_1}{2\omega} \right) + \frac{c_3 g_3^2}{25\omega} \right] + \frac{\varepsilon_2^{(r)}}{10} \left[\frac{c_1 c_3 g_1^2}{2\Delta_1} + c_2 g_2^2 \left(\frac{c_3}{\Delta_1} + \frac{c_1}{9\omega} \right) + \frac{c_3 g_3^2}{\Delta_1} \right] \right\},$$

$$\mathcal{J}_{0,2}^{(4)} \approx \frac{g_1 g_2}{2\omega}\left\{\varepsilon_1^{(r)}\left[-\frac{c_1 g_1^2 + c_2 g_2^2}{2\Delta_1\Delta_2\Delta_3} + \frac{g_3^2}{\omega^2}\left(\frac{c_1 c_2}{\omega} + \frac{c_3\Delta_3}{4\Delta_1\Delta_2}\right)\right] + \varepsilon_2^{(r)}\left[\frac{c_1 g_1^2}{8\Delta_1\omega^2} + \frac{c_2 g_2^2}{2\Delta_1\Delta_2\Delta_3} + \frac{g_3^2}{\omega}\left(c_3\frac{\Delta_1 - \Delta_2}{3\Delta_1\Delta_2\Delta_3} - \frac{c_1 c_2}{2\omega^2}\right)\right]\right\},$$

(B2)

$$\mathcal{A}_{0,2}^{(4)} \approx \frac{g_1 g_2}{20\omega^4}\left\{\frac{\varepsilon_1^{(r)}}{2}\left[c_1 c_2(g_1^2 + g_2^2) - c_3 g_3^2\left(\frac{1}{3} - c_1 c_2\right)\right] - \varepsilon_2^{(r)}\left[c_1 c_2\left(\frac{g_1^2}{10} + \frac{g_2^2}{3}\right) - \frac{c_3 g_3^2}{5}\left(\frac{1}{3} - c_1 c_2\right)\right]\right\}.$$

(B3)

[1] E. T. Jaynes and F. W. Cummings, Proc. IEEE **51**, 89 (1963).

[2] Q. Xie, H. Zhong, M. T. Batchelor, and C. Lee, J. Phys. A **50**, 113001 (2017).

[3] D. Braak, Phys. Rev. Lett. **107**, 100401 (2011).

[4] Q.-H. Chen, C. Wang, S. He, T. Liu, and K.-L. Wang, Phys. Rev. A **86**, 023822 (2012).

[5] D. Leibfried, R. Blatt, C. Monroe, and D. Wineland, Rev. Mod. Phys. **75**, 281 (2003).

[6] P. Forn-Diaz, J. Lisenfeld, D. Marcos, J. J. Garcia-Ripoll, E. Solano, C. J. P. M. Harmans, and J. E. Mooij, Phys. Rev. Lett. **105**, 237001 (2010).

[7] P. Forn-Diaz, G. Romero, C. J. P. M. Harmans, E. Solano, and J. E. Mooij, Sci. Rep. **6**, 26720 (2016).

[8] P. Forn-Diaz, J. J. Garcia-Ripoll, B. Peropadre, J.-L. Orgiazzi, M. A. Yurtalan, R. Belyansky, C. M. Wilson, and A. Lupascu, Nat. Phys. **13**, 39 (2017).

[9] Z. Chen, Y. Wang, T. Li, L. Tian, Y. Qiu, K. Inomata, F. Yoshihara, S. Han, F. Nori, J. S. Tsai, and J. Q. You, Phys. Rev. A **96**, 012325 (2017).

[10] X. Gu, A. F. Kockum, A. Miranowicz, Y. X. Liu, and F. Nori, Phys. Rep. **718-719**, 1 (2017).

[11] T. Niemczyk, F. Deppe, H. Huebl, E. P. Menzel, F. Hocke, M. J. Schwarz, J. J. Garcia-Ripoll, D. Zueco, T. Hummer, E. Solano, A. Marx, and R. Gross, Nat. Phys. **6**, 772 (2010).

[12] F. Yoshihara, T. Fuse, S. Ashhab, K. Kakuyanagi, S. Saito, and K. Semba, Nat. Phys. **13**, 44 (2017).

[13] J. Casanova, G. Romero, I. Lizuain, J. J. Garcia-Ripoll, and E. Solano, Phys. Rev. Lett. **105**, 263603 (2010).

[14] O. Di Stefano, R. Stassi, L. Garziano, A. Frisk Kockum, S. Savasta and F. Nori, New J. Phys. **19**, 053010 (2017).

[15] J. Casanova, R. Puebla, H. Moya-Cessa, and M. B. Plenio, npj Quantum Inf. **4**, 47 (2018).

[16] I. Travenec, Phys. Rev. A **85**, 043805 (2012).

[17] V. V. Albert, G. D. Scholes, and P. Brumer, Phys. Rev. A **84**, 042110 (2011).

[18] L. Duan, Y.-F. Xie, D. Braak, and Q.-H. Chen, J. Phys. A **49**, 464002 (2016).

[19] E. Lupo, A. Napoli, A. Messina, E. Solano, and I. L. Egusquiza, arXiv:1807.08674.

[20] E. Barnes and S. Das Sarma, Phys. Rev. Lett. **109**, 060401 (2012).

[21] B. Sriram Shastry, J. Phys. A **38**, L431 (2005).

[22] H. K. Owusu and E. A. Yuzbashyan, J. Phys. A **44**, 395302 (2011).

[23] D. Chruściński, A. Messina, B. Militello, and A. Napoli, Phys. Rev. A **91**, 042123 (2015).

[24] L. D. Landau, Phys. Z. Sowjetunion **2**, 46 (1932).

[25] C. Zener, Proc. R. Soc. London, Ser. A **137**, 696 (1932).

[26] E. C. G. Stückelberg, Helv. Phys. Acta **5**, 369 (1932).

[27] E. Majorana, Nuovo Cimento **9**, 43 (1932).

[28] S. Fishman, K. Mullen, and E. Ben-Jacob, Phys. Rev. A **42**, 5181 (1990).

[29] N. V. Vitanov and K.-A. Suominen, Phys. Rev. A **59**, 4580 (1999).

[30] A. V. Shytov, Phys. Rev. A **70**, 052708 (2004).

[31] M. Scala, B. Militello, A. Messina, and N. V. Vitanov, Phys. Rev. A **84**, 023416 (2011).

[32] A. V. Dodonov, B. Militello, A. Napoli, and A. Messina, Phys. Rev. A **93**, 052505 (2016).

[33] K. Bergmann, H. Theuer, and B. W. Shore, Rev. Mod. Phys. **70**, 1003 (1998).

[34] P. Kral, I. Thanopulos, and M. Shapiro, Rev. Mod. Phys. **79**, 53 (2007).

[35] N. V. Vitanov, A. A. Rangelov, B. W. Shore, and K. Bergmann, Rev. Mod. Phys. **89**, 015006 (2017).

[36] S. Schiemann, A. Kuhn, S. Steuerwald, and K. Bergmann, Phys. Rev. Lett. **71**, 3637 (1993).

[37] N. V. Vitanov and S. Stenholm, Phys. Rev. A **56**, 1463 (1997).

[38] M. Scala, B. Militello, A. Messina, and N. V. Vitanov, Opt. Spectrosc. **111**, 589 (2011).

[39] B. Militello, M. Scala, A. Messina, and N. V. Vitanov, Phys. Scr., T **2011**, 014019 (2011).

[40] F. L. Traversa, M. Di Ventra, and F. Bonani, Phys. Rev. Lett. **110**, 170602 (2013).

[41] M. Moskalets and M. Büttiker, Phys. Rev. B **66**, 205320 (2002).

[42] J. H. Shirley, Phys. Rev. **138**, B979 (1965).

[43] A. V. Dodonov, J. Phys.: Conf. Ser. **161**, 012029 (2009).

[44] S. De Liberato, D. Gerace, I. Carusotto, and C. Ciuti, Phys. Rev. A **80**, 053810 (2009).

[45] I. M. de Sousa and A. V. Dodonov, J. Phys. A **48**, 245302 (2015).

[46] D. S. Veloso and A. V. Dodonov, J. Phys. B **48**, 165503 (2015).

[47] L. C. Monteiro and A. V. Dodonov, Phys. Lett. A **380**, 1542 (2016).

[48] A. V. Dodonov, J. J. Díaz-Guevara, A. Napoli, and B. Militello, Phys. Rev. A **96**, 032509 (2017).

[49] H. Dessano and A. V. Dodonov, Phys. Rev. A **98**, 022520 (2018).

[50] M. B. Plenio, Phys. Rev. Lett. **95**, 090503 (2005).

[51] A. Peres, Phys. Rev. Lett. **77**, 1413 (1996).

[52] M. Horodecki, P. Horodecki, and R. Horodecki, Phys. Lett. A **223**, 1 (1996).

[53] Y.-X. Liu, J. Q. You, L. F. Wei, C. P. Sun, and F. Nori, Phys. Rev. Lett. **95**, 087001 (2005).

[54] Y.-X. Liu, H.-C. Sun, Z. H. Peng, A. Miranowicz, J. S. Tsai, and F. Nori, Sci. Rep. **4**, 7289 (2014).

[55] Y.-J. Zhao, J.-H. Ding, Z. H. Peng, and Y.-X. Liu, Phys. Rev. A **95**, 043806 (2017).

[56] P. Zhao, X. Tan, H. Yu, S.-L. Zhu, and Y. Yu, Phys. Rev. A **96**, 043833 (2017).

[57] J. Majer, J. M. Chow, J. M. Gambetta, J. Koch, B. R. Johnson, J. A. Schreier, L. Frunzio, D. I. Schuster, A. A. Houck, A. Wallraff, A. Blais, M. H. Devoret, S. M. Girvin, and R. J. Schoelkopf, Nature (London) **449**, 443 (2007).

[58] M. Hofheinz, H. Wang, M. Ansmann, R. C. Bialczak, E. Lucero, M. Neeley, A. D. O'Connell, D. Sank, J. Wenner, J. M. Martinis, and A. N. Cleland, Nature (London) **459**, 546 (2009).

[59] L. DiCarlo, J. M. Chow, J. M. Gambetta, L. S. Bishop, B. R. Johnson, D. I. Schuster, J. Majer, A. Blais, L. Frunzio, S. M. Girvin, and R. J. Schoelkopf, Nature (London) **460**, 240 (2009).

[60] J. Li, M. P. Silveri, K. S. Kumar, J.-M. Pirkkalainen, A. Vepsäläinen, W. C. Chien, J. Tuorila, M. A. Sillanpää, P. J. Hakonen, E. V. Thuneberg, and G. S. Paraoanu, Nat. Commun. **4**, 1420 (2013).

[61] S. J. Srinivasan, A. J. Hoffman, J. M. Gambetta, and A. A. Houck, Phys. Rev. Lett. **106**, 083601 (2011).

[62] Y. Chen *et al.*, Phys. Rev. Lett. **113**, 220502 (2014).

[63] S. Zeytinoğlu, M. Pechal, S. Berger, A. A. Abdumalikov, Jr., A. Wallraff, and S. Filipp, Phys. Rev. A **91**, 043846 (2015).

[64] In the numeric examples we set $\phi_k^{(j)} = 0$ and $w_k^{(j)} = 1$, unless stated otherwise. Besides, the time modulation of $g_{k,l}$ can be incorporated straightforwardly in our formalism.

[65] A. V. Dodonov, D. Valente, and T. Werlang, Phys. Rev. A **96**, 012501 (2017).

[66] F. Beaudoin, J. M. Gambetta, and A. Blais, Phys. Rev. A **84**, 043832 (2011).

[67] H. Paik, D. I. Schuster, L. S. Bishop, G. Kirchmair, G. Catelani, A. P. Sears, B. R. Johnson, M. J. Reagor, L. Frunzio, L. I. Glazman, S. M. Girvin, M. H. Devoret, and R. J. Schoelkopf, Phys. Rev. Lett. **107**, 240501 (2011).

[68] J. M. Fink, R. Bianchetti, M. Baur, M. Göppl, L. Steffen, S. Filipp, P. J. Leek, A. Blais, and A. Wallraff, Phys. Rev. Lett. **103**, 083601 (2009).

[69] M. Neeley, R. C. Bialczak, M. Lenander, E. Lucero, M. Mariantoni, A. D. O'Connell, D. Sank, H. Wang, M. Weides, J. Wenner, Y. Yin, T. Yamamoto, A. N. Cleland, and J. M. Martinis, Nature (London) **467**, 570 (2010).

[70] L. DiCarlo, M. D. Reed, L. Sun, B. R. Johnson, J. M. Chow, J. M. Gambetta, L. Frunzio, S. M. Girvin, M. H. Devoret, and R. J. Schoelkopf, Nature (London) **467**, 574 (2010).

[71] K. Kakuyanagi, Y. Matsuzaki, C. Déprez, H. Toida, K. Semba, H. Yamaguchi, W. J. Munro, and S. Saito, Phys. Rev. Lett. **117**, 210503 (2016).

[72] M. Reagor, W. Pfaff, C. Axline, R. W. Heeres, N. Ofek, K. Sliwa, E. Holland, C. Wang, J. Blumoff, K. Chou, M. J. Hatridge, L. Frunzio, M. H. Devoret, L. Jiang, and R. J. Schoelkopf, Phys. Rev. B **94**, 014506 (2016).

[73] N. Ofek, A. Petrenko, R. Heeres, P. Reinhold, Z. Leghtas, B. Vlastakis, Y. Liu, L. Frunzio, S. M. Girvin, L. Jiang, M. Mirrahimi, M. H. Devoret, and R. J. Schoelkopf, Nature (London) **536**, 441 (2016).

[74] Y. Lu, S. Chakram, N. Leung, N. Earnest, R. K. Naik, Z. Huang, P. Groszkowski, E. Kapit, J. Koch, and D. I. Schuster, Phys. Rev. Lett. **119**, 150502 (2017).